Journal of Metals, Materials and Minerals, Vol. 32, No. 1, pp. 48-54, 2022

Facile synthesis of heterostructured g-C_3N_4/Ag -TiO_2 photocatalysts with enhanced visible-light photocatalytic performance

Chonnipha TANGWONGPUTTI[1], Prasert REUBROYCHAROEN[2], and Pornapa SUJARIDWORAKUN[3,*]

[1] *Department of Materials Science, Faculty of Science, Chulalongkorn University, Bangkok 10330, Thailand*
[2] *Department of Chemical Technology, Faculty of Science, Chulalongkorn University, Bangkok 10330, Thailand*
[3] *Center of Excellence on Petrochemical and Materials Technology, Chulalongkorn University, Bangkok, 10330, Thailand*

***Corresponding author e-mail:** pornapa.s@chula.ac.th

Received date:
22 November 2021
Revised date
15 January 2022
Accepted date:
17 January 2022

Keywords:
g-C_3N_4/Ag-TiO_2;
Surface plasmon resonance;
Heterojunction;
Visible light

Abstract

In this study, the g-C_3N_4/Ag-TiO_2 composite photocatalysts were prepared to enhance the efficient utilization of solar energy. The g-C_3N_4 was synthesized by facile heat treatment of urea at 600°C for 4 h, and 0.05 wt% to 3 wt% Ag-TiO_2 were obtained through the chemical reduction method. The composite photocatalysts were prepared by mixing the g-C_3N_4 and Ag-TiO_2 with a weight ratio of 50:50 at room temperature. The photocatalytic efficiency was carried out by using 0.05 g of photocatalysts with 10 mg·L^{-1} of rhodamine B 120 mL under 60 min of visible light irradiation. The experimental results indicated that a sample with 0.1 wt% Ag-TiO_2 could degrade rhodamine B up to 21.21%. The g-C_3N_4/(0.1 wt% Ag-TiO_2) and g-C_3N_4 showed rhodamine B degradation efficiency up to 100%, which was 10.4 times and 4.7 times of pure TiO_2 and 0.1 wt% Ag-TiO_2, respectively. It can be suggested that the Ag deposited on TiO_2 played an important role in the absorption capability under the visible light through the surface plasmon resonance effect. In addition, heterojunction between g-C_3N_4 and TiO_2 could reduce the recombination of electron-hole pairs.

1. Introduction

Nowadays, the photocatalytic process can enhance the efficient utilization of solar energy and degrade water pollutants into carbon dioxide and water, simultaneously. Anatase titanium dioxide (TiO_2) is the most widely used as a photocatalyst due to its high photocatalytic efficiency, low toxicity, low cost, and chemical inertness [1,2]. However, TiO_2 has a high recombination rate of electron-hole pairs because of its wide band gap (3.2 eV). In addition, the photocatalytic reaction can be excited by UV which has only 4% of incoming sunlight [3]. To overcome these limitations of TiO_2, Ag deposited on TiO_2 (Ag-TiO_2) plays an important role in the absorption capability under the visible light through the surface plasmon resonance effect. The excited electron flow from the silver to the conduction band of TiO_2 ($Ag \rightarrow Ag^+ + e^-$) [4-7]. Graphitic carbon nitride (g-C_3N_4) has attracted great attention in photocatalytic applications, for example, the degradation of organic pollutants [8-13], carbon dioxide reduction into energy fuels [14-16], hydrogen production [11,17], and nitrogen fixation [18]. g-C_3N_4 has been simply prepared by one-step calcination of melamine [15,19] or urea [9] at 400°C to 600°C. In addition, g-C_3N_4 has a narrow band gap (2.7 eV) which responds to visible light at 400 nm to 450 nm [10].

From the previous research, Deliang *et al.* [5] reported the Ag-TiO_2 synthesis by photoreduction of silver nitrate ($AgNO_3$). The Ag^0 was deposited on TiO_2 (P25) surface in the mixed solution of ethylene glycol and ethanol by UV irradiation. The rhodamine B degradation was reported in terms of first-order kinetics. The decomposition rate of 1 wt% Ag-TiO_2 was 0.11 min^{-1}, which was 22 times of TiO_2 (P25) under visible light irradiation for 30 min. Mengqiao *et al.* [12] synthesized g-C_3N_4/(Ag-TiO_2) by dispersing g-C_3N_4 and Ag-TiO_2 with a mass ratio of 1:1 into DI water by ultrasonication for 3 h. Then, the mixture was dried and calcined at 400°C for 1 h. Rhodamine B degradation was analyzed through decomposition rate. g-C_3N_4/(Ag-TiO_2) had a decomposition rate at 0.0983 min^{-1} which was 6.3, 2.2, and 1.63 times of TiO_2, Ag-TiO_2, and g-C_3N_4, respectively under visible light irradiation for 30 min. Furthermore, the stability of photocatalysts was important for practical use. Photodegradation of rhodamine B with the reusing ability after 5 cycles of Ag-TiO_2, g-C_3N_4, and g-C_3N_4/Ag-TiO_2 photocatalysts under visible-light irradiation was reported [5,9,12].

In this research, we aim to enhance the photocatalytic activity under visible light irradiation, which is the highest component of sunlight (about 43%) [19]. The optimum Ag loading amount and photocatalytic efficiency for rhodamine B degradation under visible-light irradiation of Ag-TiO_2, g-C_3N_4, and g-C_3N_4/Ag-TiO_2 composite photocatalysts were studied.

2. Experimental

2.1 Materials

Urea ($CO(NH_2)_2$, AR.grade, Qrec) was used to synthesize the g-C_3N_4 sheet. Anatase titanium dioxide (TiO_2, 99%) was purchased from KRONOS Worldwide, Inc. Silver nitrate ($AgNO_3$, 99.5%, Merck)

was used as an Ag precursor. Polyvinylpyrrolidone (PVP, 99%, Sigma-Aldrich) and sodium borohydride ($NaBH_4$, 98.5%, Chem-Supply) were used as a stabilizer and reducing agent, respectively. Rhodamine B (RhB, Loba Chemie) was used as the target pollutant.

2.2 Preparation of photocatalysts

g-C_3N_4 was prepared by calcination of 10 g urea at 600°C, 4 h with a heating rate of 5°C·min^{-1} in a muffle furnace [9]. To synthesize Ag-TiO_2, starting by dissolving $AgNO_3$ which was used as Ag precursor at 0.05 wt% to 3 wt% in DI water. Next, PVP solution which acted as the dispersant was added to the Ag solution. Then, the Ag-PVP solution was slowly added to the suspension of TiO_2. After that, $NaBH_4$ was slightly added into the Ag-PVP-TiO_2 suspension to reduce Ag ions through the chemical reduction method from Equation (1) [7]:

$$AgNO_3 + NaBH_4 + 3H_2O \rightarrow Ag + H_3BO_3 + NaNO_3 + \frac{7}{2} H_2 \quad (1)$$

Finally, the suspension was stirred for 1 h and dried at 110°C, respectively [20]. g-C_3N_4/(Ag-TiO_2) composite photocatalysts were obtained by mixing g-C_3N_4 and 0.1 wt% Ag-TiO_2 with a weight ratio of 50:50 in DI water. To completely disperse, the suspension was stirred for 15 min and sonicated for 15 min, respectively [21]. Finally, the suspension was centrifuged and dried at 60°C to remove the remaining water [12].

2.3 Characterizations

X-ray diffraction (XRD; Bruker, D8 Advance, Germany) with Cu Kα radiation (λ = 1.5406 Å) was used to determine the crystalline phase of the prepared photocatalysts. The crystallite size was calculated using the Scherrer equation by Equation (2) [8].

$$D = \frac{k\lambda}{\beta cos\theta} \quad (2)$$

Where D was the average crystallite size (nm), k was the dimensionless shape factor = 0.9, λ was the X-ray wavelength = 0.15406 (nm), β was the full width at half maximum (radians), θ was Bragg-diffraction angle (radians).

Photoluminescence (PL) spectra were studied at room temperature on a fluorescence spectrometer (PerkinElmer LS 55) with an excitation wavelength of 325 nm.

The specific surface area, pore size, and pore volume of samples were analyzed using a surface area and porosimetry analyzer (Micromeritics, 3Flex 3500) at 77 K. Before analyzing, the samples were degassed at 300°C for 12 h under vacuum. The specific surface area was determined by Brunauer-Emmett-Teller (BET). Pore size and pore volume were calculated by Barrett-Joyner-Halenda (BJH) which appropriated with mesopore range.

Morphology and structure were obtained using a transmission electron microscope (TEM, JEOL JEM-1400) at 120 kV.

2.4 Photocatalytic efficiency evaluation

Photocatalytic efficiency was examined by rhodamine B degradation under a visible light source (120 mW·cm^{-2}, 300 W Xe lamp with UV cutoff filter). The distance between the sample and the light source was equal to 20 cm. 0.05 g photocatalyst was dispersed into 10 ppm rhodamine B 120 mL by ultrasonic wave for 5 min. Before the light irradiation, the suspension was stirred in dark for 30 min to reach the adsorption-desorption equilibrium. The solution was collected 5 mL every 10 min from both under dark and light irradiation. Then, the solution was centrifuged to remove catalyst and analyzed concentration by UV–Vis spectrophotometer (Perkin Elmer Lambda 35) at the maximum absorbance wavelength 554 nm. The dye degradation efficiency of all samples was compared in terms of C/C_0 (mg·L^{-1}) and time (min) and calculated in terms of efficiency (%) by Equation (3-4):

$$Dye\ adsorption\ efficiency\ (\%) = \frac{C_0 - C_D}{C_0} \times 100 \quad (3)$$

$$Dye\ degradation\ efficiency\ (\%) = \frac{C_D - C}{C_D} \times 100 \quad (4)$$

Where C_0 was the initial concentration (mg·L^{-1}), C_D was the dye concentration after keeping in dark (mg·L^{-1}), C was the dye concentration at each irradiated time (mg·L^{-1}).

3. Results and discussion

3.1 Crystallographic Information

XRD patterns of pristine TiO_2, 0.1 wt% Ag-TiO_2, g-C_3N_4, and g-C_3N_4/(0.1 wt% Ag-TiO_2) composite photocatalysts were shown in Figure 1. The diffraction peaks at around 25.3° (101), 37.8° (004), 48.2° (200), 54.0° (105), 55.2° (211), 62.7° (204), 68.9° (116), 70.3° (220), 75.1° (215) observed in TiO_2, 0.1 wt% Ag-TiO_2 and g-C_3N_4/(0.1 wt% Ag-TiO_2) were lattice planes of anatase TiO_2 (JCPDS card no. 21-1272) [22]. Due to the ionic radius of Ag^+ ion being larger than that of Ti^{4+} ion, thus Ag^+ tended to be observed on TiO_2 surface instead of being incorporated into TiO_2 lattice sites [23,24]. The characteristic peaks of Ag were not appeared for 0.1 wt% Ag-TiO_2 sample due to its low contents or high dispersity [12,20]. For g-C_3N_4, the diffraction peaks at 13.1° (100) and 27.4° (002) could be attributed to in-plane structural packing of tri-s-triazine repeating units and graphite-like

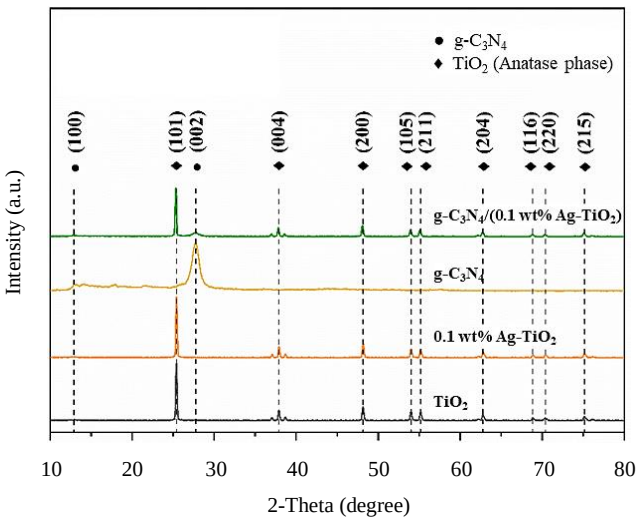

Figure 1. XRD patterns of TiO_2, 0.1 wt% Ag-TiO_2, g-C_3N_4, and g-C_3N_4/(0.1 wt% Ag-TiO_2) composite photocatalysts.

stacking, respectively (JCPDS Card No. 87-1526) [9,12,22]. which would enhance the rate of electron transfer on the surface of the catalyst [10]. It was shown that the g-C_3N_4/(0.1 wt% Ag-TiO_2) composite photocatalysts consisted of the characteristic peak of both g-C_3N_4 and Ag-TiO_2. In addition, the phase structures and peak position of the TiO_2 and g-C_3N_4 were not changed after composite preparation. The crystallite size of pristine TiO_2, TiO_2 in the Ag-TiO_2 and g-C_3N_4/(0.1 wt% Ag-TiO_2) calculated by the Scherrer equation (Equation (2)), were about 42.4, 41.7, and 41.4, respectively. It was demonstrated that the crystallite size of TiO_2 had almost not changed.

3.2 Photoluminescence emission

The recombination of electron-hole pairs which is considered to be the major factor that affects photocatalytic performance was investigated by the photoluminescence (PL) emission. Low PL intensity indicates the low recombination of electron-hole pairs and high photocatalytic efficiency, respectively. Figure 2 showed that the g-C_3N_4 had strong PL intensity at 455 nm as a result of the transition of lone pair electron to the π^* conduction band [25]. While the composite with a weight ratio of g-C_3N_4:0.1 wt% Ag-TiO_2 at 50:50 had lower PL intensity compared with pure g-C_3N_4 at 455 nm because of electron transfer from electron conduction bridge of Ag and heterojunction between g-C_3N_4 and TiO_2 [22]. The maximum wavelength of about 390 nm, Ag-TiO_2, and g-C_3N_4/(Ag-TiO_2) had lower intensity than pure TiO_2. It indicated that a heterostructured composite could reduce electron-hole recombination and enhance the efficiency of TiO_2.

3.3 Nitrogen adsorption-desorption

The specific surface area, pore size, and pore volume of samples were analyzed by nitrogen adsorption-desorption isotherm as shown in Figure 3. Mesopores in the samples were verified by hysteresis loop type IV and BJH calculation [10]. From Table 1, BET specific surface area of TiO_2, 0.1 wt% Ag-TiO_2, g-C_3N_4, g-C_3N_4/(0.1 wt% Ag-TiO_2) were 7.84, 8.31, 94.39, 42.91 $m^2 \cdot g^{-1}$, respectively. g-C_3N_4 had the highest specific surface area which corresponded to the highest dye adsorption efficiency in the dark as shown in Figure 7.

3.4 Morphology and structure

TEM images of TiO_2, g-C_3N_4, and g-C_3N_4/(0.1 wt% Ag-TiO_2) were shown in Figure 4. Figure 4(a) displayed the agglomeration of TiO_2 particles with spherical-like morphology. For g-C_3N_4, it had the thin layer and lamellar structure as shown in Figure 4(b). The g-C_3N_4/(0.1 wt% Ag-TiO_2) composite was illustrated in Figure 4(c) composed of the spherical-like particle of TiO_2 dispersed on the g-C_3N_4 sheet.

3.5 Band potential determination

The band potentials of photocatalyst were used to describe the photocatalytic mechanism. Which calculated using the following equations [13,26]:

$$E_{VB} = \chi + 0.5E_g - E^e \quad (5)$$

$$E_{CB} = E_{VB} - E_g \quad (6)$$

Where E_{VB} and E_{CB} were the valence band and conduction band potential, respectively χ was the absolute electronegativity of

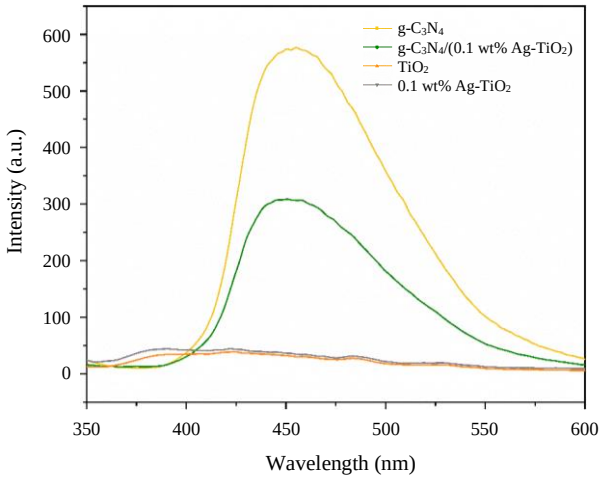

Figure 2. PL spectra of g-C_3N_4, g-C_3N_4/(0.1 wt% Ag-TiO_2), TiO_2, and 0.1 wt% Ag-TiO_2 composite photocatalysts.

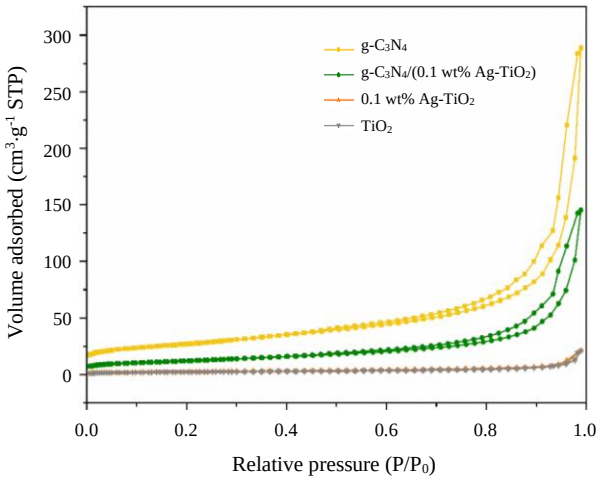

Figure 3. Nitrogen adsorption-desorption isotherm of TiO_2, 0.1 wt% Ag-TiO_2, g-C_3N_4, and g-C_3N_4/(0.1 wt% Ag-TiO_2) with a weight ratio of 50:50.

Table 1. The specific surface area, pore size, and pore volume of TiO_2 and prepared photocatalysts.

Type of photocatalysts	S_{BET} ($m^2 \cdot g^{-1}$)	BJH Pore size (nm)	BJH Pore volume ($cm^3 \cdot g^{-1}$)
TiO_2	7.84	20.29	0.0318
0.1 wt% Ag-TiO_2	8.31	16.60	0.0330
g-C_3N_4	94.39	19.63	0.4426
g-C_3N_4/(0.1 wt% Ag-TiO_2)	42.91	19.98	0.2251

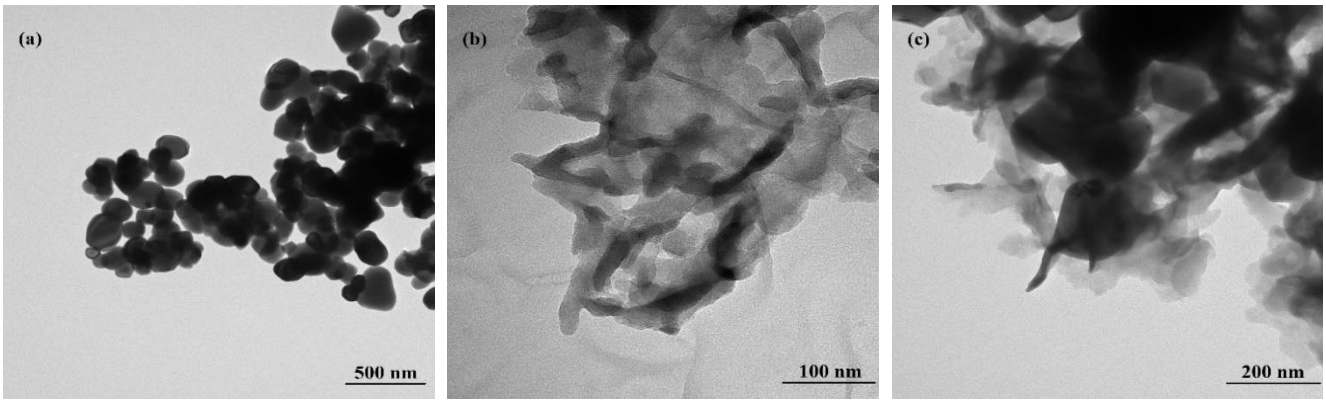

Figure 4. TEM images of (a) TiO_2 (50,000x), (b) g-C_3N_4 (300,000x), and (c) g-C_3N_4/(0.1 wt% Ag-TiO_2) with a weight ratio of 50:50 (150,000x).

constituent atoms of semiconductor (TiO_2 = 5.81 eV [27], g-C_3N_4 = 4.73 eV [28]). E_g was the band gap energy of semiconductor (Anatase TiO_2 = 3.28 eV [29], g-C_3N_4 = 2.82 eV [9]). E^e was the energy of free electron on hydrogen scale (4.5 eV). The values of E_{VB} and E_{CB} of TiO_2 and g-C_3N_4 was shown in Table 2.

3.6 Photocatalytic efficiency

The photocatalytic efficiency of TiO_2 and Ag-TiO_2 with various Ag loading contents (0.05 wt% to 3 wt%) were tested under the simulated visible light irradiation for 60 min as shown in Figure 5. The result shows that, the 0.1 wt% Ag-TiO_2 sample showed the highest RhB dye degradation efficiency at 21.21%, which is 2.2 times higher than that of pure TiO_2 under the same condition. The deposition of Ag on the TiO_2 surface with the optimum condition could enhance the dye degradation efficiency due to the surface plasmon resonance effect [5,6]. When the surface plasmon band of Ag absorbed the visible light, the excited electron would transfer to the conduction band of TiO_2 ($Ag \rightarrow Ag^+ + e^-$) [4] and increase the oxidation molecules to degrade the organic dye, respectively [30]. On the other hand, at higher silver content (0.2 wt% to 3 wt%), the photocatalytic efficiency trended to decrease because of the agglomeration of Ag particles which would block the reaction site at the TiO_2 surface [31] and act as a recombination center, resulting in reduced photoactivity [32].

The correlation between C/C_0 and time of TiO_2, Ag-TiO_2, g-C_3N_4, and composite photocatalyst was shown in Figure 6. The results indicated that the rhodamine B dye was stable under visible irradiation while it was degraded in the presence of photocatalyst samples. The Ag-TiO_2 exhibited higher performance than pure TiO_2, in that both of TiO_2 and 0.1 wt% Ag-TiO_2 could not completely degrade RhB dye within the range of studied time (60 min). While g-C_3N_4/(0.1 wt% Ag-TiO_2) composite and g-C_3N_4 completely degraded RhB dye within 30 min and 20 min, respectively. It was shown that the photocatalytic efficiency obtained from this work was higher than that of previous reports [10,12,33]. As demonstrated in Figure 6 and Figure 7, g-C_3N_4 and g-C_3N_4/(0.1 wt% Ag-TiO_2) composite performed high degradation efficiency due to the effect of the high dye adsorption ability and suitable band gap energy for visible-light absorption of g-C_3N_4. As the results, the dye degradation efficiency of 0.1 wt% Ag-TiO_2 was 21.21% which was 2.2 times higher than pure TiO_2 (9.62%). The g-C_3N_4/(0.1 wt% Ag-TiO_2) and g-C_3N_4 had dye degradation efficiency at 100% which was 10.4 times and 4.7 times of TiO_2 and Ag-TiO_2, respectively under visible light irradiation for 60 min. It was suggested that the improved photocatalytic activity of the composite would be further studied by varying and finding the optimum ratio between g-C_3N_4 and Ag-TiO_2.

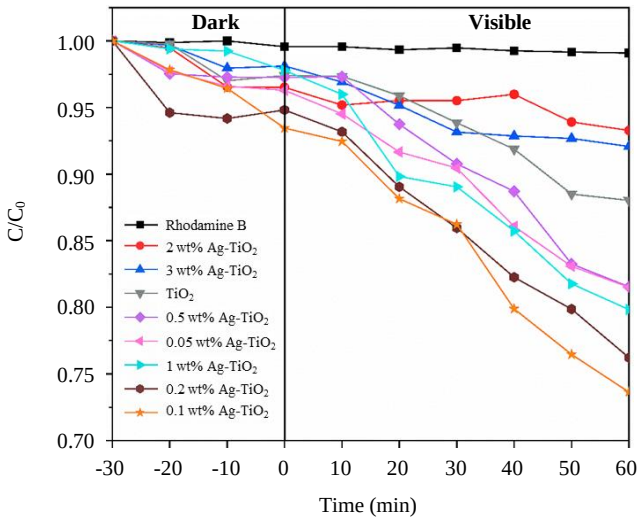

Figure 5. The correlation between C/C_0 and time of TiO_2 and 0.05 wt% to 3 wt% Ag-TiO_2 composite photocatalysts under visible light irradiation for 60 min.

Table 2. Absolute electronegativity (χ), band gap energy (E_g), valence band potential (E_{VB}), and conduction band potential (E_{CB}) of TiO_2 and g-C_3N_4 photocatalysts.

Photocatalysts	χ (eV)	E_g (eV)	E_{VB} (eV)	E_{CB} (eV)
TiO_2	5.81	3.28	2.95	-0.33
g-C_3N_4	4.73	2.82	1.64	-1.18

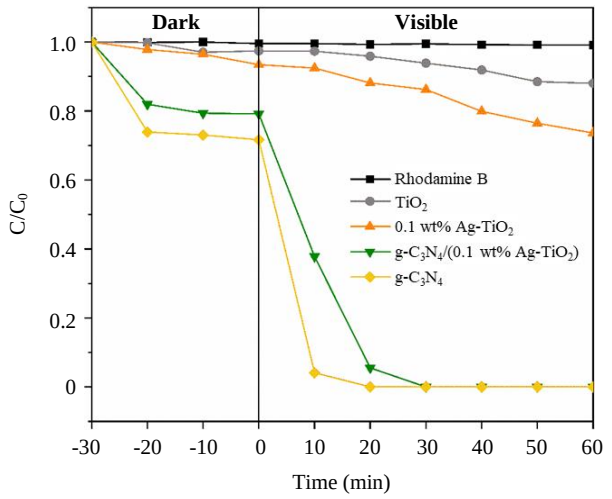

Figure 6. The correlation between C/C_0 and time of TiO_2, 0.1 wt% Ag-TiO_2, g-C_3N_4/(0.1 wt% Ag-TiO_2) with a weight ratio of 50:50, and g-C_3N_4 under visible light irradiation for 60 min.

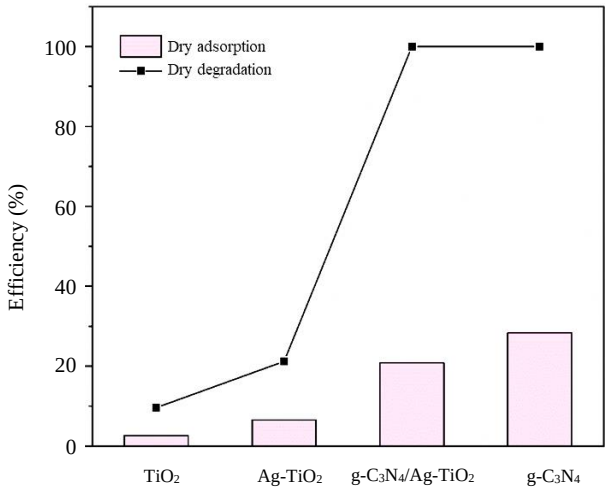

Figure 7. The comparison of dye adsorption efficiency (%) after keeping in dark for 30 min and dye degradation efficiency (%) under visible light irradiation for 60 min of TiO_2, 0.1 wt% Ag-TiO_2, g-C_3N_4/(0.1 wt% Ag-TiO_2) and g-C_3N_4 photocatalysts.

The photocatalytic mechanism of g-C_3N_4/Ag-TiO_2 composite photocatalysts was proposed in Figure 8. The conduction band and valence band of g-C_3N_4 was a higher potential than TiO_2 therefore it was suitable for the formation of heterojunction with TiO_2. When g-C_3N_4 absorbed and excited under the visible-light irradiation, the photogenerated electron at the conduction band of g-C_3N_4 (-1.18) would generally go down to the lower conduction band potential of TiO_2 (-0.33). As a result, the recombination of electron-hole pairs was decreased [10,12,34]. At the same time, the deposited Ag nanoparticles responded to visible light which could produce electrons by surface plasmon resonance effect and also served as electron conduction bridge to transfer the electron from g-C_3N_4 to the conduction band of TiO_2 [33]. These photogenerated electrons (e^-(CB)) could be trapped by O_2 in an aqueous solution to produce free radical, e.g., superoxide ($O_2^{-\cdot}$), hydroperoxyl radical ($HOO^\cdot$), and $OH^\cdot$ radical. Then, $OH^\cdot$ radical reacted with dye to become CO_2 and H_2O [35] by the following equations:

$$O_2 + e^-(CB) \rightarrow O_2^{-\cdot}(ads) \quad (7)$$

$$O_2^{-\cdot}(ads) + H^+ \leftrightarrow HOO^\cdot(ads) \quad (8)$$

$$2HOO^\cdot(ads) \rightarrow H_2O_2(ads) + O_2 \quad (9)$$

$$H_2O_2(ads) \rightarrow 2OH^\cdot(ads) \quad (10)$$

$$Dye + OH^\cdot \rightarrow CO_2 + H_2O \quad (11)$$

The photogenerated hole (h^+(VB)) at the valence band of g-C_3N_4 directly reacted with dye by themselves [12,36] to generate the oxidation products as shown in the equation:

$$Dye + h^+(VB) \rightarrow oxidation\ products \quad (12)$$

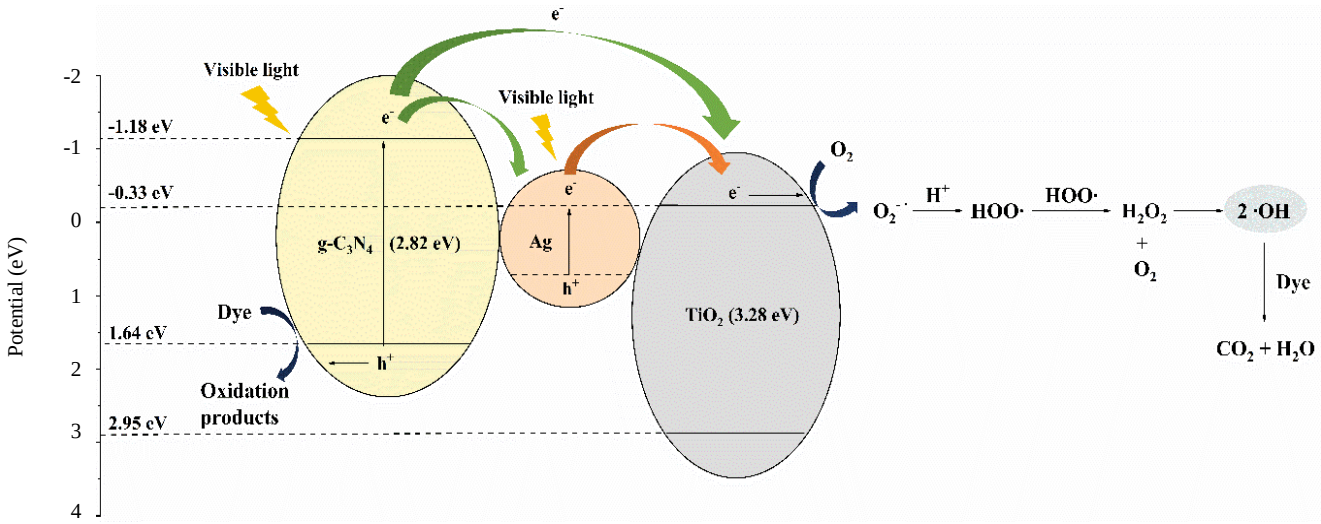

Figure 8. Possible photocatalytic mechanism of g-C_3N_4/Ag-TiO_2 composite photocatalysts under visible light irradiation.

4. Conclusions

In this study, the enhanced photocatalytic activity under visible light of Ag-TiO_2 photocatalysts was performed. The highest photocatalytic activity for degradation of RhB dye of Ag-TiO_2 photocatalyst was obtained from sample loading with 0.1 wt% Ag. The photodegradation efficiency under visible light irradiation of the composite composed of g-C_3N_4 and 0.1 wt% Ag-TiO_2 at a weight ratio of 50:50 was 10.4 times and 4.7 times higher than the pristine TiO_2 and 0.1 wt% Ag-TiO_2, respectively. The high photocatalytic performance of the composite under visible light was caused by the following aspects: (1) visible light absorption of narrow band gap from g-C_3N_4, and through surface plasmon resonance effect from Ag (2) high dye adsorption ability of g-C_3N_4 (3) retarding of recombination of photogenerated carriers by electron conduction bridge of Ag and heterojunction structure. In summary, this study may offer the facile method for preparing Ag-TiO_2 and g-C_3N_4/Ag-TiO_2 composite photocatalysts to remediate the organic pollutant in wastewater under visible-light excitation.

Acknowledgements

The authors acknowledge financial support by the GAICCE Research Grant from ASEAN University Network/Southeast Asia Engineering Education Development Network (AUN/SEED-net), and the Scholarship from the Graduate School, Chulalongkorn University to commemorate the 72nd anniversary of his Majesty King Bhumibol Adulyadej is gratefully acknowledged. In addition, we are also thankful to Metallurgy and Materials Science Research Institute (MMRI) Chulalongkorn University for the research facility and equipment.

References

[1] M. Pelaez, N. T. Nolan, S. C. Pillai, M. K. Seery, P. Falaras, A. G. Kontos, P. S. M. Dunlop, J. W. J. Hamilton, J. A. Byrne, K. O'Shea, M. H. Entezari, and D. D. Dionysiou, "A review on the visible light active titanium dioxide photocatalysts for environmental applications," *Applied Catalysis B: Environmental,* vol. 125, pp. 331-349, 2012.

[2] C. Su, C. M. Tseng, L. F. Chen, B. H. You, B. C. Hsu, and S. S. Chen, "Sol–hydrothermal preparation and photocatalysis of titanium dioxide," *Thin Solid Films,* vol. 498, no. 1-2, pp. 259-265, 2006.

[3] J. Wen, J. Xie, X. Chen, and X. Li, "A review on g-C_3N_4-based photocatalysts," *Applied Surface Science,* vol. 391, pp. 72-123, 2017.

[4] C. Gunawan, W. Y. Teoh, C. P. Marquis, J. Lifia, and R. Amal, "Reversible Antimicrobial Photoswitching in Nanosilver," *Small,* vol. 5, no. 3, pp. 341-344, 2009.

[5] D. Chen, Q. Chen, L. Ge, L. Yin, B. Fan, H. Wang, H. Lu, H. Xu, R. Zhang, and G. Shao, "Synthesis and Ag-loading-density-dependent photocatalytic activity of Ag@TiO_2 hybrid nanocrystals," *Applied Surface Science,* vol. 284, pp. 921-929, 2013.

[6] K. H. Leong, B. L. Gan, S. Ibrahim, and P. Saravanan, "Synthesis of surface plasmon resonance (SPR) triggered Ag/TiO_2 photocatalyst for degradation of endocrine disturbing compounds," *Applied Surface Science,* vol. 319, pp. 128-135, 2014.

[7] M. Stucchi, C. L. Bianchi, C. Argirusis, V. Pifferi, B. Neppolian, G. Cerrato, and D. C. Boffito, "Ultrasound assisted synthesis of Ag-decorated TiO_2 active in visible light," *Ultrason Sonochem,* vol. 40, no. Pt A, pp. 282-288, 2018.

[8] R. Fagan, D. E. McCormack, S. J. Hinder, and S. C. Pillai, "Photocatalytic properties of g-C_3N_4-TiO_2 heterojunctions under UV and visible light conditions," *Materials (Basel),* vol. 9, no. 4, 2016.

[9] T. Narkbuakaew, and P. Sujaridworakun, "Synthesis of Tri-S-Triazine Based g-C_3N_4 Photocatalyst for Cationic Rhodamine B Degradation under Visible Light," *Topics in Catalysis,* vol. 63, no. 11, pp. 1086-1096, 2020.

[10] G. Sui, J. Li, L. Du, Y. Zhuang, Y. Zhang, Y. Zou, and B. Li, "Preparation and characterization of g-C_3N_4/Ag–TiO_2 ternary hollowsphere nanoheterojunction catalyst with high visible light photocatalytic performance," *Journal of Alloys and Compounds,* vol. 823, p. 153851, 2020.

[11] Y. Xing, X. Wang, S. Hao, X. Zhang, X. Wang, W. Ma, G. Zhao, and X. Xu, "Recent advances in the improvement of g-C_3N_4 based photocatalytic materials," *Chinese Chemical Letters,* vol. 32, no. 1, pp. 13-20, 2021.

[12] M. Zang, L. Shi, L. Liang, D. Li, and J. Sun, "Heterostructured g-C_3N_4/Ag–TiO_2 composites with efficient photocatalytic performance under visible-light irradiation," *RSC Advances,* vol. 5, no. 69, pp. 56136-56144, 2015.

[13] J. Zhang, Y. Hu, X. Jiang, S. Chen, S. Meng, and X. Fu, "Design of a direct Z-scheme photocatalyst: preparation and characterization of Bi_2O_3/g-C_3N_4 with high visible light activity," *J Hazard Mater,* vol. 280, pp. 713-22, 2014.

[14] Z. Sun, H. Wang, Z. Wu, and L. Wang, "g-C_3N_4 based composite photocatalysts for photocatalytic CO_2 reduction," *Catalysis Today,* vol. 300, pp. 160-172, 2018.

[15] D. O. Adekoya, M. Tahir, and N. A. S. Amin, "g-C_3N_4/(Cu/TiO_2) nanocomposite for enhanced photoreduction of CO_2 to CH_3OH and HCOOH under UV/visible light," *Journal of CO_2 Utilization,* vol. 18, pp. 261-274, 2017.

[16] S. Singh, A. Modak, and K. K. Pant, "CO_2 Reduction to Methanol Using a Conjugated Organic–Inorganic Hybrid TiO_2–C_3N_4 Nano-assembly," *Transactions of the Indian National Academy of Engineering,* vol. 6, no. 2, pp. 395-404, 2021.

[17] J. Wang, J. Huang, H. Xie, and A. Qu, "Synthesis of g-C_3N_4/TiO_2 with enhanced photocatalytic activity for H_2 evolution by a simple method," *International Journal of Hydrogen Energy,* vol. 39, no. 12, pp. 6354-6363, 2014.

[18] G. Zhao, and X. Xu, "Cocatalysts from types, preparation to applications in the field of photocatalysis," *Nanoscale,* vol. 13, no. 24, pp. 10649-10667, 2021.

[19] Z. Zou, J. Ye, K. Sayama, and H. Arakawa, "Direct splitting of water under visible light irradiation with an oxide semiconductor photocatalyst," *Nature,* vol. 414, no. 6864, pp. 625-7, 2001.

[20] T. Narkbuakaew, and P. Sujaridworakul, "Enhancement of Photocatalytic Performance of Anatase by Silver Deposition through Chemical Reduction Process at Room Temperature," *Materials Science Forum,* vol. 998, pp. 71-77, 2020.

[21] Y. Liu, S. Wu, J. Liu, S. Xie, and Y. Liu, "Synthesis of g-C_3N_4/TiO_2 nanostructures for enhanced photocatalytic reduction of U(vi) in water," *RSC Advances,* vol. 11, no. 8, pp. 4810-4817, 2021.

[22] R. Geng, J. Yin, J. Zhou, T. Jiao, Y. Feng, L. Zhang, Y. Chen, Z. Bai, and Q. Peng, "In Situ Construction of Ag/TiO_2/g-C_3N_4 Heterojunction Nanocomposite Based on Hierarchical Co-Assembly with Sustainable Hydrogen Evolution," *Nanomaterials (Basel)*, vol. 10, no. 1, 2019.

[23] X. Gao, B. Zhou, and R. Yuan, "Doping a metal (Ag, Al, Mn, Ni and Zn) on TiO_2 nanotubes and its effect on Rhodamine B photocatalytic oxidation," *Environmental Engineering Research*, vol. 20, no. 4, pp. 329-335, 2015.

[24] J. Vargas Hernández, S. Coste, A. García Murillo, F. Carrillo Romo, and A. Kassiba, "Effects of metal doping (Cu, Ag, Eu) on the electronic and optical behavior of nanostructured TiO_2," *Journal of Alloys and Compounds*, vol. 710, pp. 355-363, 2017.

[25] P. Xia, B. Cheng, J. Jiang, and H. Tang, "Localized π-conjugated structure and EPR investigation of g-C_3N_4 photocatalyst," *Applied Surface Science*, vol. 487, pp. 335-342, 2019.

[26] Q. Yuan, L. Chen, M. Xiong, J. He, S.-L. Luo, C.-T. Au, and S.-F. Yin, "Cu_2O/$BiVO_4$ heterostructures: synthesis and application in simultaneous photocatalytic oxidation of organic dyes and reduction of Cr(VI) under visible light," *Chemical Engineering Journal*, vol. 255, pp. 394-402, 2014.

[27] H. Y. Hafeez, S. K. Lakhera, N. Narayanan, S. Harish, Y. Hayakawa, B. K. Lee, and B. Neppolian, "Environmentally Sustainable Synthesis of a $CoFe_2O_4$-TiO_2/rGO Ternary Photocatalyst: A Highly Efficient and Stable Photocatalyst for High Production of Hydrogen (Solar Fuel)," *ACS Omega*, vol. 4, no. 1, pp. 880-891, 2019.

[28] J. Liu, "Origin of High Photocatalytic Efficiency in Monolayer g-C_3N_4/CdS Heterostructure: A Hybrid DFT Study," *The Journal of Physical Chemistry C*, vol. 119, no. 51, pp. 28417-28423, 2015.

[29] T. Narkbuakaew, and P. Sujaridworakun, "Role of Ag (0) deposited on TiO_2 nanoparticles for superior photocatalytic performance induced by calcination," *Optical Materials*, vol. 98, p. 109407, 2019.

[30] Q. Zhang, D. Q. Lima, I. Lee, F. Zaera, M. Chi, and Y. Yin, "A highly active titanium dioxide based visible-light photocatalyst with nonmetal doping and plasmonic metal decoration," *Angew Chem Int Ed Engl*, vol. 50, no. 31, pp. 7088-7092, 2011.

[31] S. I. Mogal, V. G. Gandhi, M. Mishra, S. Tripathi, T. Shripathi, P. A. Joshi, and D. O. Shah, "Single-Step Synthesis of Silver-Doped Titanium Dioxide: Influence of Silver on Structural, Textural, and Photocatalytic Properties," *Industrial & Engineering Chemistry Research*, vol. 53, no. 14, pp. 5749-5758, 2014.

[32] Y. Wu, H. Liu, J. Zhang, and F. Chen, "Enhanced Photocatalytic Activity of Nitrogen-Doped Titania by Deposited with Gold," *The Journal of Physical Chemistry C*, vol. 113, no. 33, pp. 14689-14695, 2009.

[33] Y. Chen, W. Huang, D. He, Y. Situ, and H. Huang, "Construction of Heterostructured g-C_3N_4/Ag/TiO_2 Microspheres with Enhanced Photocatalysis Performance under Visible-Light Irradiation," *ACS Applied Materials & Interfaces*, vol. 6, no. 16, pp. 14405-14414, 2014.

[34] J. Ge, Y. Zhang, Y.-J. Heo, and S.-J. Park, "Advanced Design and Synthesis of Composite Photocatalysts for the Remediation of Wastewater: A Review," *Catalysts*, vol. 9, no. 2, p. 122, 2019.

[35] A. Ajmal, I. Majeed, R. N. Malik, H. Idriss, and M. A. Nadeem, "Principles and mechanisms of photocatalytic dye degradation on TiO_2 based photocatalysts: a comparative overview," *RSC Adv.*, vol. 4, no. 70, pp. 37003-37026, 2014.

[36] S. Zhao, S. Chen, H. Yu, and X. Quan, "g-C_3N_4/TiO_2 hybrid photocatalyst with wide absorption wavelength range and effective photogenerated charge separation," *Separation and Purification Technology*, vol. 99, pp. 50-54, 2012.